

EGF-IL2 bispecific and bivalent EGF fusion toxin efficacy against syngeneic head and neck cancer mouse models

YUE QIU^{1,2}, ZENG QI^{3,4}, ZHAOHUI WANG^{3,4}, YU CAO^{1,5}, LING LU¹, HUIPING ZHANG^{3,4},
DAVID MATHES³, ELIZABETH A. POMFRET⁴, SHI-LONG LU¹ and ZHIRUI WANG^{3,4}

¹Department of Otolaryngology-Head and Neck Surgery, School of Medicine, University of Colorado Anschutz Medical Campus, Aurora, CO 80045, USA; ²Department of Immunology, College of Basic Medical Sciences, China Medical University, Shenyang, Liaoning 110122, P.R. China; Divisions of ³Plastic and Reconstructive Surgery and ⁴Transplant Surgery, Department of Surgery, School of Medicine, University of Colorado Anschutz Medical Campus, Aurora, CO 80045, USA; ⁵Department of Breast Surgery, The First Hospital of China Medical University, Shenyang, Liaoning 110001, P.R. China

Received August 15, 2022; Accepted December 1, 2022

DOI: 10.3892/or.2022.8474

Abstract. The epidermal growth factor receptor (EGFR) remains one of the best molecules for developing targeted therapy for multiple human malignancies, including head and neck squamous cell carcinoma (HNSCC). Small molecule inhibitors or antibodies targeting EGFR have been extensively developed in recent decades. Immunotoxin (IT)-based therapy, which combines cell surface binding ligands or antibodies with a peptide toxin, represents another cancer treatment option. A total of 3 diphtheria toxin (DT)-based fusion toxins that target human EGFR-monovalent EGFR IT (mono-EGF-IT), bivalent EGFR IT (bi-EGF-IT), and a bispecific IT targeting both EGFR and interleukin-2 receptor (bis-EGF/IL2-IT) were recently generated by the authors. Improved efficacy and reduced toxicity of bi-EGF-IT compared with mono-EGF-IT in immunocompromised HNSCC mouse models was reported. In the present study, bis-EGF/IL2-IT were generated using a unique DT-resistant yeast expression system and evaluated the *in vitro* and *in vivo* efficacy and toxicity of the 3 EGF-ITs in immunocompetent mice. The results demonstrated that while the three EGF-ITs had different efficacies *in vitro* and *in vivo*

against HNSCC, bi-EGF-IT and bis-EGF/IL2-IT had significantly improved *in vivo* efficacy and remarkably less off-target toxicity compared with mono-EGF-IT. In addition, bis-EGF/IL2-IT was superior to bi-EGF-IT in reducing tumor size and prolonging survival in the metastatic model. These data suggested that targeting either the tumor immune microenvironment or enhancing the binding affinity could improve the efficacy of IT-based therapy. Bi-EGF-IT and bis-EGF/IL2-IT represent improved candidates for IT-based therapy for future clinical development.

Introduction

Head and neck squamous cell carcinoma (HNSCC) comprise a heterogeneous group of cancers derived from the oral cavity, nasopharynx, oropharynx, hypopharynx, and larynx (1). An estimated 65,000 new cases of HNSCC are diagnosed each year in the USA, where it is the seventh most common cancer (2). Tobacco, alcohol consumption, and human papillomavirus (HPV) infection are known risk factors for HNSCC (3-5). HNSCC remains a lethal disease despite concerted efforts to improve treatment options, including surgery, chemotherapy, targeted therapy and immunotherapy (1,6-8). The 5-year survival rate for HNSCC decreases drastically with cancer stage, from ~80% in early stages (I-II) to only ~40% for advanced stages (III-IV) (9-11).

The epidermal growth factor receptor (EGFR) remains the best molecule for HNSCC-targeted therapy, given its high frequency of overexpression in this disease, regardless of stage or HPV status (12-14). Targeting EGFR with either an antibody (e.g., cetuximab) or small molecule inhibitor (e.g., erlotinib) has been extensively investigated in clinical trials and has been approved by the FDA for the treatment of patients with advanced HNSCC (7,15-18). However, clinical efficacy is modest, and acquired resistance to EGFR inhibitors often occurs over time (1,7,19,20). Thus, additional therapeutics with improved efficacy that could potentially overcome this resistance are urgently needed (21,22).

Correspondence to: Dr Zhirui Wang, Division of Plastic and Reconstructive Surgery, Department of Surgery, School of Medicine, University of Colorado Anschutz Medical Campus, 12700 E 19th Avenue, Aurora, CO 80045, USA
E-mail: zhirui.wang@cuanschutz.edu

Dr Shi-Long Lu, Department of Otolaryngology-Head and Neck Surgery, School of Medicine, University of Colorado Anschutz Medical Campus, 12700 E 19th Avenue Aurora, CO 80045, USA
E-mail: shi-long.lu@cuanschutz.edu

Key words: monovalent, bivalent, bispecific, human EGF fusion toxin, interleukin-2, diphtheria toxin, syngeneic head and neck squamous cell carcinoma mouse models

Immunotoxin (IT)-based therapy combines cell surface binding ligands or antibody-based single-chain fragment variable (scFv) with a peptide toxin and represents another cancer treatment option (23-25). A novel bivalent diphtheria toxin (DT)-based EGF fusion toxin (bi-EGF-IT) with improved efficacy and remarkably less off-target toxicity than the monovalent EGF-IT (mono-EGF-IT) in human HNSCC cell lines and HNSCC mouse models established in immunocompromised mice was recently developed by the authors (26). In the present study, the efficacy and toxicity of human bi-EGF-IT was further evaluated in immunocompetent mice in the presence of host immunity. CD25 is highly expressed on the surface of tumor-infiltrating effector regulatory T cells (Tregs) (27). It was hypothesized that a bispecific fusion toxin containing both EGF and interleukin-2 (bis-EGF/IL2-IT) would achieve a dual advantage for treatment of EGFR⁺ HNSCC via both EGF-based targeted therapy and IL2-based immunotherapy (via Treg depletion). In addition, IL-2 (Aldesleukin, PROLEUKIN[®]) was the first FDA-approved cancer immunotherapy to stimulate immune system for metastatic renal cell carcinoma in 1992 and melanoma in 1998 and was approved as a combination treatment for neuroblastoma in 2015 (28). Based on the aforementioned information, a bis-EGF/IL2-IT was generated and it was compared with other two EGF fusion toxins, i.e., mono-EGF-IT and bi-EGF-IT in immunocompetent mice in the presence of host immunity.

Materials and methods

DNA construct for the bispecific human EGF/IL2 fusion toxin. Codon-optimized human IL2 DNA was synthesized by GenScript with a *Bam*HI site at the N-terminus and an *Eco*RI site at the C-terminus. This DNA replaced the second human EGF in the bivalent human EGF fusion toxin DNA construct (bi-EGF-IT) between the *Bam*HI and *Eco*RI sites, yielding the bispecific human EGF-IL2 fusion toxin DNA construct (bis-EGF/IL2-IT). The human EGF domain and human IL2 were linked by three tandem G₄S linkers (G₄S)₃. A tag of 6 histidines (6 x His tag) was added to the C terminus to facilitate protein purification (Fig. 1).

Expression of the bispecific human EGF/IL2 fusion toxin. The human EGF/IL2-IT DNA construct was linearized and transformed into the DT-resistant *Pichia pastoris* yeast strain (29) using the Gene Pulser Xcell Electroporation System (Bio-Rad Laboratories, Inc.). The transformed cells were spread onto YPD agar plates (1% yeast extract, 2% peptone, 1.5% agar and 2% dextrose) containing 100 µg/ml zeocin and incubated at 30°C for 3-4 days. A total of 6 colonies were randomly picked and cultured in 5 ml YPD medium at 30°C for 24 h with shaking at 250 rpm and then in YPG medium (1% yeast extract, 2% peptone, 1% glycerol) for another 24 h. The induction of EGF/IL2-IT was carried out in 2 ml BMMYC medium (1% yeast extract, 2% peptone, 100 mM potassium phosphate, pH 7.0, 1.34% yeast nitrogen base without amino acids, 4x10⁻³% biotin, 0.5% methanol, and 1% casamino acids) for 48 h at 25°C with shaking at 225 rpm. Methanol (0.5%) was added twice daily to maintain the methanol level. Antifoam (Emerald Performance Materials LLC) was added to all growth and induction media at a concentration of 0.02%.

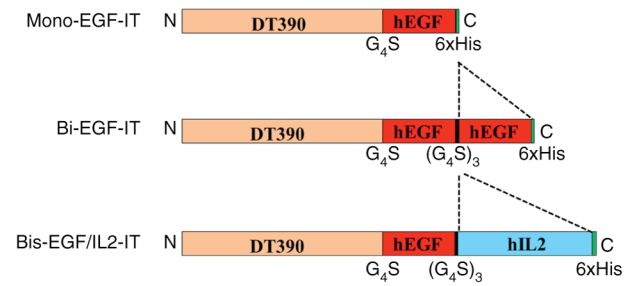


Figure 1. Schematic diagrams of the 3 EGF fusion toxins. Mono-EGF-IT, monovalent human EGF fusion toxin; bi-EGF-IT, bivalent human EGF fusion toxin; bis-EGF/IL2-IT, bispecific human EGF/IL2 fusion toxin; DT, diphtheria toxin; hEGF, human epidermal growth factor; hIL2, human interleukin-2; G₄S, four glycine residues and one serine residue; His, histidine; N, N-terminal; C, C-terminal.

Phenylmethylsulfonyl fluoride (PMSF, 1 mM; MilliporeSigma) was added to inhibit protein degradation during the induction phase. Penicillin (100 U/ml) and streptomycin (100 µg/ml) were added to all growth and induction media to inhibit bacterial contamination. The culture supernatants were analyzed using 4-12% SDS-PAGE gels. One human bis-EGF/IL2-IT clone was selected for large-scale expression. The Excella E24 incubator shaker (Eppendorf) was used for large-scale expression. The seed culture was prepared by inoculating a single colony into YPD medium and then incubating at 25°C overnight with shaking at 225 rpm. Next, 5% of the seed culture was transferred to 1-L PYREX shake flasks containing 250 ml YPD medium and cultured at 30°C and 250 rpm for 24 h. The cells were centrifuged at 491 x g for 5 min, and the cell pellet was resuspended in 250 ml YPG medium and cultured at 30°C for 24 h with shaking at 250 rpm. For the induction phase, the cells were centrifuged at 491 x g for 5 min, and the cell pellet was resuspended in 125 ml BMMYC induction medium and induced at 25°C for 48 h with shaking at 225 rpm. Methanol (0.5%) was added twice daily to maintain the methanol level. After the induction, the yeast cells were pelleted by centrifugation at 1,692 x g for 10 min at 4°C. The supernatant was used for first-step protein purification. Antifoam, PMSF, and penicillin/streptomycin were added to the expression medium, as described for the small-scale preparation.

Purification of the bispecific human EGF/IL2 fusion toxin. First-step purification of bis-EGF/IL2-IT was carried out using Ni-Sepharose[™] 6 fast flow resin. The resin was packed in an XK50 column (Cytiva), equilibrated with 20 mM Tris-HCl (pH 7.4), 0.5 M NaCl, and 5 mM imidazole. The sample was loaded onto the equilibrated column in the same buffer. The column was washed with this buffer, and then the bound proteins were eluted with 20 mM Tris-HCl pH 7.4, 0.5 M NaCl and 500 mM imidazole. The purification fractions were analyzed using 4-12% SDS-PAGE gels. The fractions containing bis-EGF/IL2-IT were pooled and dialyzed against 20 mM Tris-HCl pH 8.0, 1 mM EDTA, and 5% glycerol using Spectra/Por membrane tubing with a 3.5 kDa cut-off (Repligen) at 4°C with stirring. The dialysis buffer was replaced once. Strong anion exchange resin Poros 50 HQ (Applied Biosystems; Thermo Fisher Scientific, Inc.) was packed in an XK16/20 column (Cytiva) for second-step purification. The

column was equilibrated with 20 mM Tris-HCl pH 8.0, 1 mM EDTA, and 5% glycerol. The dialyzed sample was loaded onto the column and washed with the same buffer. The bound protein was eluted with 100- and 200-mM sodium borate, then 200 mM sodium borate plus 50 mM NaCl (250 mM total salt) in 20 mM Tris-HCl pH 8.0, 1 mM EDTA, and 5% glycerol. The purified fractions were analyzed using 4-12% SDS-PAGE gels. The fractions containing the human bis-EGF/IL2-IT were pooled and dialyzed using Spectra/Por membrane tubing (3.5 kDa cut-off) against PBS plus 5% glycerol at 4°C with stirring. The dialysis buffer was replaced once. The protein concentration was measured using the Pierce BCA Protein Assay Kit (Thermo Fisher Scientific, Inc.). Mono-EGF-IT, bi-EGF-IT, DT390 (truncated DT), and anti-murine PD-1 IT (mPD1-IT) were also expressed and purified using the same DT-resistant yeast *Pichia pastoris* expression system (26).

Biotin-labeling of the three EGF fusion toxins. The 3 EGF fusion toxins (mono-EGF-IT, bi-EGF-IT, and bis-EGF/IL2-IT) were labeled with EZ-Link Sulfo-NHS Biotin (Thermo Fisher Scientific, Inc.). NHS-Biotin (1 mg) was added to 1 mg of each of the 3 EGF fusion toxins, and the mixtures were incubated for 2 h at 4°C with shaking. The samples were transferred to a Slide-A-Lyzer dialysis cassette (10 kDa MWCO, 0.5-3 ml, Thermo Fisher Scientific, Inc.) and dialyzed against 1X PBS for 24 h at 4°C with stirring. The dialysis buffer was replaced once.

Cells, western blotting, and antibodies. The murine EGFR⁺ HNSCC tumor cell line MOC2, established from a carcinogen-induced oral SCC in a C57BL/6 mouse (30), was purchased from Kerafast, Inc. The cell line was authenticated by STR (short tandem repeat) and was free of pathogens. Purified fusion toxins were analyzed using 4-12% SDS-PAGE gels. The gels were stained with Gel Code Blue Staining Reagent (Thermo Fisher Scientific, Inc.) and mounted with DryEase Mini Cellophane (Thermo Fisher Scientific, Inc.). Western blot analysis was performed as previously described (31). Briefly, proteins (~1 µg in 15 µl per sample) were separated on 4-12% SDS-PAGE gels and transferred onto nitrocellulose membranes (Thermo Fisher Scientific, Inc.). The membranes were blocked with 5% blotting grade blocker non-fat dry milk (Bio-Rad Laboratories, Inc.) in 1X PBS, 0.02% Tween 20 for 1 h with shaking and washed once with 1X PBS, pH 7.4, 0.2% Tween 20 at room temperature with shaking. The three EGF fusion toxins were detected using mouse anti-DT, mouse anti-human EGF, or mouse anti-human IL2 primary antibodies (1:1,000) and rat anti-mouse IgG-HRP as the secondary antibody (1:4,000). The proteins were detected using the TMB (Tetramethylbenzidine) membrane peroxidase substrate (SeraCare; LGC Clinical diagnostics). The antibodies used in the present study are listed in Table SI.

The binding affinities of the three human EGF fusion toxins to murine EGFR⁺ HNSCC MOC2 cells. MOC2 cells were stained at 4°C for 30 min with biotinylated mono-EGF-IT, bi-EGF-IT, or bis-EGF/IL2-IT at a range of concentrations (0.01 to 200 nM). The biotinylated anti-human EGFR mAb (Santa Cruz Biotechnology, Inc.) was used as a positive control at a final concentration of 36 nM. Negative control cells were

stained at 4°C for 30 min only with streptavidin-PE (SA-PE) at a final concentration of 1.5 ng/µl. Flow cytometry was carried out using a CytoFLEX Flow cytometer (Beckman Coulter, Inc.), and data were analyzed using FlowJo software v10 (FlowJo LLC). Biotinylated mPD1-IT was used as a biotinylated protein control.

K_D determination. Binding of mono-EGF-IT, bi-EGF-IT or bis-EGF/IL2-IT to murine EGFR⁺ HNSCC MOC2 cells was performed using a wide range of concentrations of biotinylated mono-EGF-IT, bi-EGF-IT, or bis-EGF/IL2-IT. The K_Ds were determined from the flow cytometric data using nonlinear regression with the saturation binding equation (GraphPad Prism 9.0.0). The mean fluorescence intensities (MFI) were plotted vs. the biotinylated mono-EGF-IT, bi-EGF-IT, or bis-EGF/IL2-IT concentration. Nonlinear regression was based on the equation $Y = B_{max} \times X / (K_D + X)$, where Y=MFI at a given biotinylated EGF fusion toxin concentration after subtracting the background, X=biotinylated EGF fusion toxin concentration, and B_{max}=the maximum specific binding in the same units as Y.

In vitro efficacy. The effect of mono-EGF-IT, bi-EGF-IT, and bis-EGF/IL2-IT on the viability of murine EGFR⁺ HNSCC MOC2 cells was determined using the CellTiter-Glo[®] Luminescent Cell Viability Assay kit (Promega Corporation), as previously described (32). This assay measures the luminescence produced by ATP production from metabolically active cells. Increasing concentrations of the mono-EGF-IT, bi-EGF-IT and bis-EGF/IL2-IT cause cell death and a corresponding reduction in ATP-related fluorescence. Luminescence was measured using a BioTek Synergy LX Multi-Mode Reader. DT390 was included as negative control.

In vivo efficacy. C57BL/6 mice were purchased from Jackson Laboratories (Bar Harbor, USA). The animal experiments were approved (approval no. 00866) by the Institutional Animal Care and Use Committee (IACUC) of the University of Colorado Anschutz Medical Campus (Aurora, USA). The housing temperature was 22°C and the housing atmosphere was set at 35% humidity. The light/dark cycle was 14-10 h, respectively, (6 am to 8 pm on) and the lighting is at 50% strength unless over-ridden for 15 min durations. Standard feed provided was Envigo Teklad Global Diets 2920X (19% protein, 6% Fat). Water was freely accessed via water bottle or water valve in the cage. C57BL/6 mice (6-8 weeks old, 20-25 g) were divided into five treatment groups: i) DT390, negative control; ii) mono-EGF-IT; iii) bi-EGF-IT; iv) bis-EGF/IL2-IT and v) erlotinib, positive control at a previously reported dose (33,34). In total, 209 mice (105 males and 104 females) were used for the present study.

A total of 3 complementary syngeneic HNSCC tumor models were used to evaluate *in vivo* efficacy in immunocompetent C57BL/6 mice, including subcutaneous (SC) tumors, orthotopic tongue SCC, and experimental metastasis models. For the SC tumor model, murine EGFR⁺ HNSCC MOC2 cells (8x10⁶ in 200 µl DMEM) were injected SC into the right flank. For the orthotopic tongue SCC model, C57BL/6 mice were anesthetized with isoflurane, and the MOC2 cells (1x10⁶ cells in 50 µl DMEM) were injected into the tongue. For the

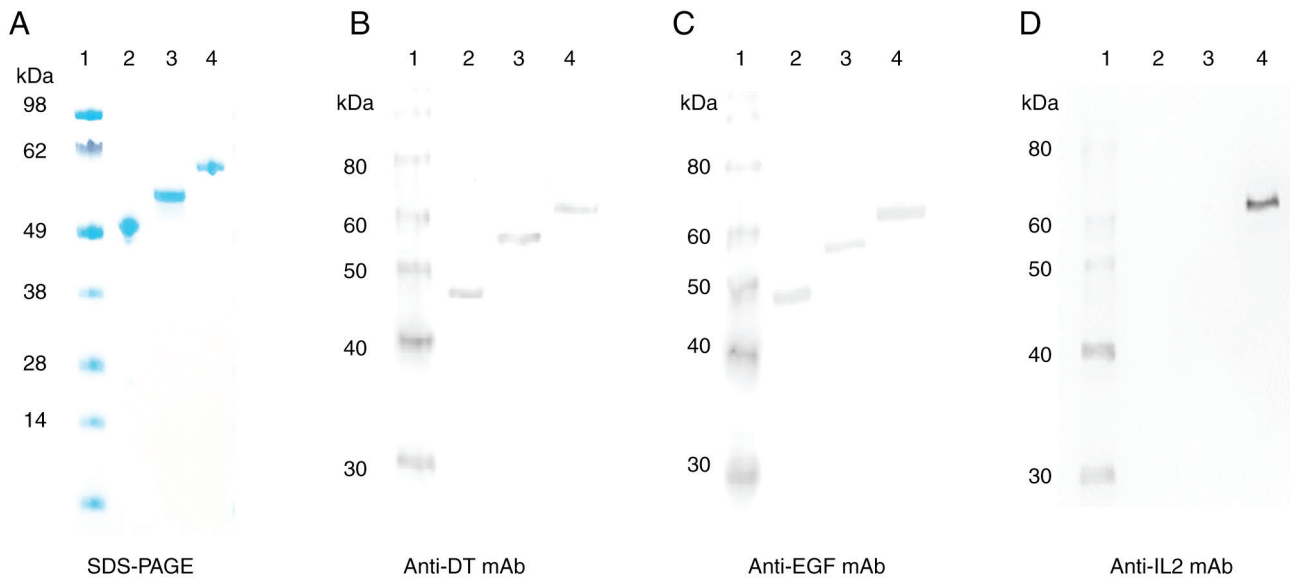


Figure 2. SDS-PAGE and western blot analysis for the three EGF fusion toxins. (A) SDS-PAGE analysis (4-12% NuPAGE). (B) Western blot analysis using a mouse anti-DT monoclonal antibody (mAb). (C) Western blot analysis using a mouse anti-human EGF mAb. (D) Western blot analysis using a mouse anti-human IL2 mAb. Lane 1: Protein marker; Lane 2: mono-EGF-IT (50.1 kDa); Lane 3: bi-EGF-IT (57.2 kDa); Lane 4: bis-EGF/IL2-IT (66.5 kDa). DT, diphtheria toxin.

experimental metastasis model, MOC2 cells (1×10^6 cells in $200 \mu\text{l}$ DMEM) were injected intravenously via the tail vein. For all 3 models, the tumor-bearing mice were randomly divided with equal sex distribution into the five treatment groups on day 3 post-inoculation.

Treatment commenced for the SC tumors and orthotopic tongue SCC on day 4 post-tumor cell inoculation of the MOC2 tumor cells and on day 10 for the experimental metastasis model. Mono-EGF-IT, bi-EGF-IT, bis-EGF/IL2-IT, or DT390 ($50 \mu\text{g}/\text{kg}$) were administered by intraperitoneal injection. Erlotinib ($20 \text{ mg}/\text{kg}$) was administered via intragastric gavage. All treatments were administered once daily for 10 consecutive days. The tumors were measured using digital Vernier calipers every 3 days, as previously described (26,35). The tumor volume was calculated according to the formula: $\text{Volume (mm}^3\text{)} = [\text{length} \times (\text{width}^2)]/2$. Quantification of lung metastases was performed by counting the number of metastases regardless of tumor size and by determining the percentage of tumor burden in 3 independent microscopic fields at $\times 5$ magnification.

The specific criteria (i.e., humane endpoints) used in the present study to determine when animals should be euthanized were: i) Tumor size reaching 2 cm in any diameter, ii) Body weight loss being over 15% compared with the littermate controls at any time point, iii) Mice reaching to moribund state or having difficulty to eat soft food or drink water, iv) Ulcerated tumors and v) Self-mutilation, hypothermia, or difficulty of breath. The maximal duration of the experiments for the present study was 3 months. The animal health and behavior were monitored once daily, and twice daily in the late stage of the experiments. Soft food such as moist chow was provided for animals in poor health condition. If their condition deteriorated further, the animals were euthanized. Mice were anesthetized with inhalation of 5% isoflurane when injection of the tumor cells to the tongues or oral gavage of

Erlotinib. The method of euthanasia used was CO_2 inhalation plus approved secondary method such as cervical dislocation and bilateral thoracotomy. After the second euthanasia method, cessation of breath and heartbeat was verified as mouse death.

Statistical analysis. IC_{50} s were determined using nonlinear regression (GraphPad Prism 9.0.0; GraphPad Software, Inc.). The P-values for the survival curves were calculated using the Mantel-Cox log-rank test (GraphPad Prism 9.0.0). The P-values for other comparisons were calculated using the unpaired two-tailed Student's t-test (GraphPad Prism 9.0.0). $P < 0.05$ was considered to indicate a statistically significant difference.

Results

Generation of the bispecific human EGF/IL2 fusion toxin. Monovalent (mono-EGF-IT) and bivalent (bi-EGF-IT) human EGF fusion toxins were previously generated using a unique DT-resistant yeast *Pichia pastoris* expression system (26). In the current study, the second human EGF was replaced by the codon-optimized human IL-2 DNA in the bi-EGF-IT DNA construct to produce the bispecific human EGF/IL2 fusion toxin (bis-EGF/IL2-IT) DNA construct (26). Bis-EGF/IL2-IT was produced using the *Pichia pastoris* expression system (26). The final purification yield of the bis-EGF/IL2-IT was $\sim 10 \text{ mg}$ per liter of harvested supernatant. Purified bis-EGF/IL2-IT was analyzed using SDS-PAGE and western blotting with monoclonal antibodies (mAb) against DT, human EGF, and human IL2. The expected molecular weight of 66.5 kDa was detected for bis-EGF/IL2-IT (Lane 4, Fig. 2A-D). Mono-EGF-IT (50.1 kDa) and bi-EGF-IT (57.2 kDa) were detected in lanes 2 and 3 when using either anti-DT or anti-human EGF mAbs (Fig. 2A-C) but not when using the anti-human IL2 mAb (Fig. 2D).

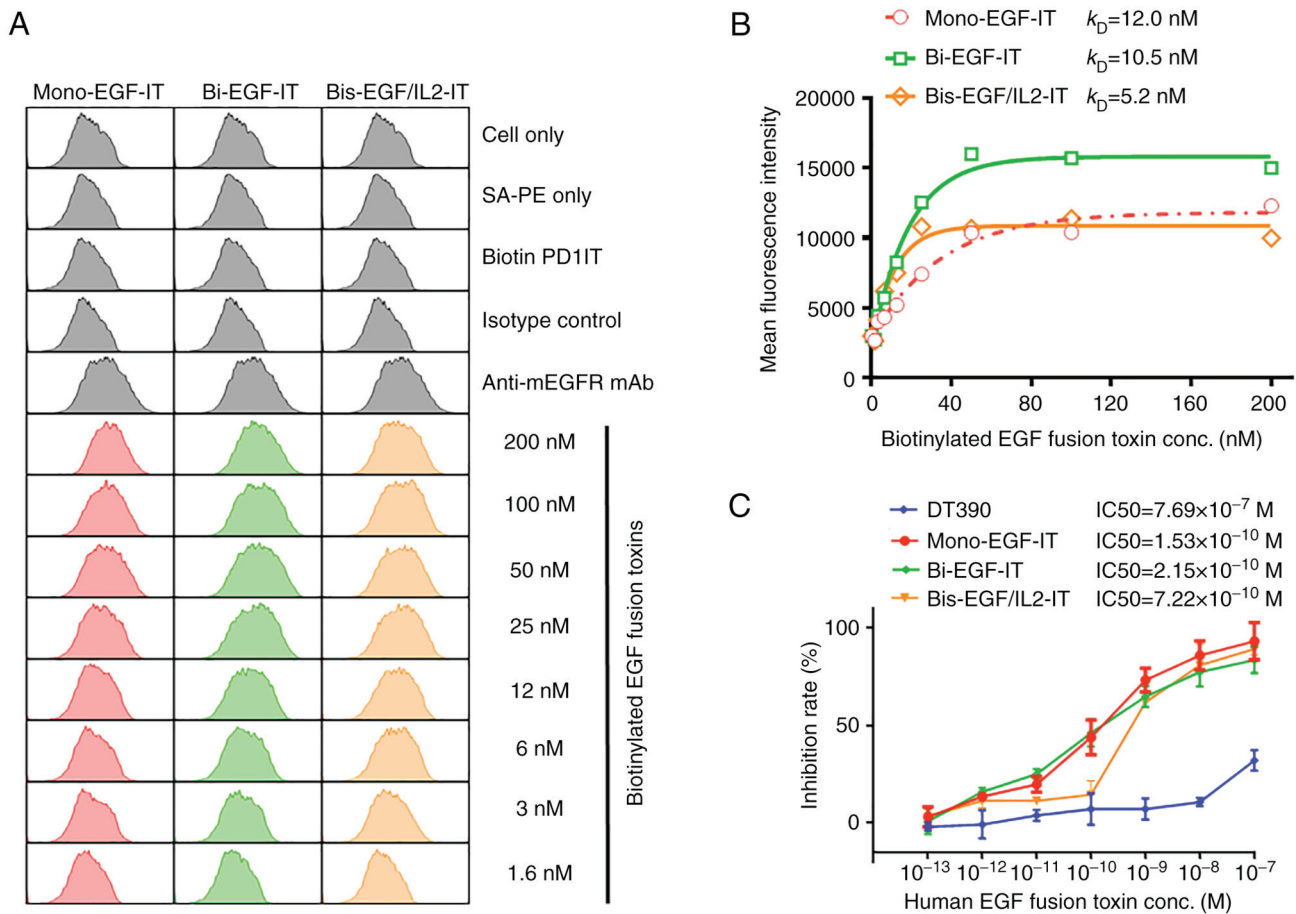


Figure 3. Binding affinity for the 3 EGF fusion toxins to murine EGFR-positive head and neck squamous cell carcinoma MOC2 cells and their effect on cell viability. (A) The binding affinities of mono-EGF-IT, bi-EGF-IT, and bis-EGF/IL2-IT to MOC2 cells were determined by flow cytometry. Negative controls included cells only, SA-PE only, biotin PD1-IT (biotinylated anti-murine PD-1 IT as control for background protein biotinylation), and an isotype control. Anti-murine EGFR mAb was used as a positive control. The data are representative of three individual experiments. (B) K_D determination for the binding of the three EGF fusion toxins to MOC2 cells. The mean fluorescence intensities from flow cytometry were plotted over a range of concentrations of biotinylated mono-EGF-IT, bi-EGF-IT, and bis-EGF/IL2-IT. The K_D s were calculated based on the nonlinear regression fit. (C) The effect of the three EGF fusion toxins on MOC2 cell viability using the CellTiter-Glo® Luminescent Cell Viability Assay (DT390, negative control, blue; mono-EGF-IT, red; bi-EGF-IT, green; bis-EGF/IL2-IT, orange). Y-axis: inhibition rate of the cell viability by determining the number of viable cells based on quantifying the ATP present. X-axis: concentrations of the three EGF fusion toxins. Cycloheximide (1.25 mg/ml) was used as a positive control. The negative control contained cells without fusion toxin. The data are from three individual experiments. The error bars indicate SD. IT, immunotoxin.

In vitro binding affinities and efficacy of the three EGF fusion toxins against murine HNSCC cells. The binding affinities of the three EGF fusion toxins were evaluated in the murine HNSCC cell line MOC2, derived from a squamous cell carcinoma of the oral cavity in a murine oral carcinogenesis model (30). MOC2 cells express EGFR (EGFR⁺), which is shown by a shift in the flow cytometric parameters using a mAb against mouse EGFR (Fig. 3). It was revealed that biotinylated mono-EGF-IT, bi-EGF-IT, and bis-EGF/IL2-IT could bind to murine MOC2 cells in a dose-dependent fashion, with a K_D of 12.0 nM for mono-EGF-IT, 10.5 nM for bi-EGF-IT, and 5.2 nM for bis-EGF/IL2-IT (Fig. 3A and B). The amino acid sequence homology is 69.81% between human and murine EGF and 62.75% between human and murine IL2.

The *in vitro* efficacy of the three EGF fusion toxins against the MOC2 cells was assessed using the CellTiter-Glo® Luminescent Cell Viability Assay. All 3 EGF fusion toxins effectively reduced cell viability of murine EGFR⁺ HNSCC MOC2 cells with IC_{50} s of 1.53×10^{-10} M, 2.15×10^{-10} M, and 7.22×10^{-10} M for mono-EGF-IT, bi-EGF-IT, and bis-EGF/

IL2-IT, respectively. The IC_{50} for the negative control DT390 was 7.69×10^{-7} M (Fig. 3C).

Efficacy of the three EGF fusion toxins against the syngeneic SC MOC2 tumor model. The *in vivo* efficacy of the three EGF fusion toxins was first evaluated using the syngeneic SC MOC2 tumor model. Beginning 4 days after tumor cell inoculation, mice were treated daily for 10 consecutive days with mono-EGF-IT, bi-EGF-IT, or bis-EGF/IL2-IT (50 μ g/kg) by intraperitoneal injection or 20 mg/kg erlotinib by intragastric gavage. The tumor-bearing mice were sacrificed on day 18, and all the tumors were collected. As demonstrated in Fig. 4, all 3 EGF fusion toxins and erlotinib significantly reduced tumor growth compared with the DT390 control group. Furthermore, bis-EGF/IL2 significantly reduced the tumor volume compared with mono-EGF-IT (Fig. 4A and B).

Efficacy of the three EGF fusion toxins against the syngeneic orthotopic tongue SCC mouse model. To mimic the clinical manifestation of HNSCC, MOC2 tumor cells was injected into

Table I. Median survival days for syngeneic tongue squamous cell carcinoma and lung metastasis mouse models following treatment.

Tumor model	Median survival days				
	DT390	Mono-EGF-IT	Bi-EGF-IT	Bis-EGF/IL2-IT	Erlotinib
Orthotopic tongue model	13	13	16.5	15	15
Lung metastasis model	19	29	47.5	41	38

IT, immunotoxin.

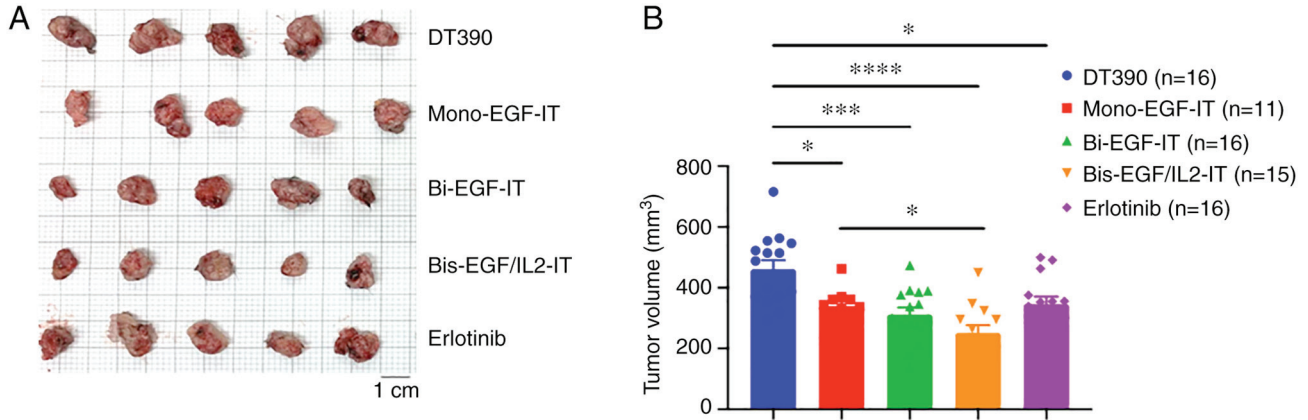


Figure 4. Antitumor efficacy of the three EGF fusion toxins against a syngeneic SC tumor model. Murine EGFR⁺ head and neck squamous cell carcinoma MOC2 cells were injected SC into the right flank. Tumor-bearing mice were treated with DT390 (negative control, n=16), mono-EGF-IT (n=11), bi-EGF-IT (n=16), bis-EGF/IL2-IT (n=15), or erlotinib (positive control, n=16) once daily for ten consecutive days beginning on day 4 after tumor cell injection. Mice were sacrificed on day 18 after tumor cell injection. (A) Images of the harvested tumors on day 18. (B) Quantification of tumor volume (mean ± SEM): DT390, 460.8±29.82; mono-EGF-IT, 339.7±16.48; bi-EGF-IT, 311.7±23.01; bis-EGF/IL2-IT, 251.5±25.19; erlotinib, 346.5±24.81. *P<0.05, ***P<0.001 and ****P<0.0001. IT, immunotoxin.

the tongues of C57BL/6 mice. Beginning 4 days after tumor cell inoculation, the mice were treated with mono-EGF-IT, bi-EGF-IT, or bis-EGF/IL2-IT (50 µg/kg) by intraperitoneal injection or 20 mg/kg erlotinib by intragastric gavage daily for ten consecutive days. Compared with DT390 and mono-EGF-IT, bi-EGF-IT, bis-EGF/IL2-IT, and erlotinib significantly prolonged the median survival time from 13 days (DT390 and mono-EGF-IT) to 15 (bis-EGF/IL2-IT, and erlotinib) or 16.5 days (bi-EGF-IT) (Fig. 5A and Table I). To further characterize the effect of the three EGF fusion toxins on murine tongue SCC tumor incidence and volume, this experiment was repeated and mice were sacrificed 9 days after tumor cell injection. At this time point, the numbers of tongue SCC tumors occurring were significantly less (1/5) in the bi-EGF-IT, bis-EGF/IL2-IT and erlotinib groups than in the mono-EGF-IT (4/5) and DT390 control groups (5/5) (Fig. 5B). Similarly, the total tongue SCC volume in the bi-EGF-IT, bis-EGF/IL2-IT, and erlotinib groups were significantly smaller than those in the mono-EGF-IT or DT390 groups (Fig. 5C).

Efficacy of the three EGF fusion toxins against lung metastasis in a syngeneic mouse model. To evaluate the effect of the three EGF fusion toxins on lung metastasis, MOC2 tumor cells were injected intravenously into C57BL/6 mice. Beginning 10 days post-tumor cell injection, mice were treated

with mono-EGF-IT, bi-EGF-IT, bis-EGF/IL2-IT, or DT390 (50 µg/kg) by intraperitoneal injection or 20 mg/kg erlotinib by intragastric gavage daily for ten consecutive days. All 3 EGF fusion toxins and erlotinib significantly prolonged the median survival time from 19 days (DT390) to 29 (mono-EGF-IT), 47.5 (bi-EGF-IT), 41 (bis-EGF/IL2-IT), or 38 (erlotinib) days (Fig. 6A and Table I). Moreover, bi-EGF-IT, bis-EGF/IL2-IT, and erlotinib were more potent than mono-EGF-IT, with bi-EGF-IT being the most efficacious (Fig. 6A).

To further assess the efficacy of the three EGF fusion toxins against metastasis, the metastasis study was repeated, and all mice were sacrificed 18 days after tumor cell inoculation. As revealed in Fig. 6B-D, the numbers and sizes of the metastases (shown as the percentage of tumor burden) in the lungs of the mice treated with bi-EGF-IT, bis-EGF/IL2-IT, or erlotinib were significantly reduced compared with the DT390 and mono-EGF-IT groups.

Comparison of mono-EGF-IT, bi-EGF-IT and bis-EGF/IL2-IT toxicity. Similar to the previous observation in NSG mice (26), C57BL/6 mice treated with mono-EGF-IT appeared generally unhealthy and lethargic compared with those treated with either bi-EGF-IT or bis-EGF/IL2-IT. The body weight of mono-EGF-IT group was declined compared with those in bi-EGF-IT and bis-EGF/IL2-IT groups although with no statistical significance

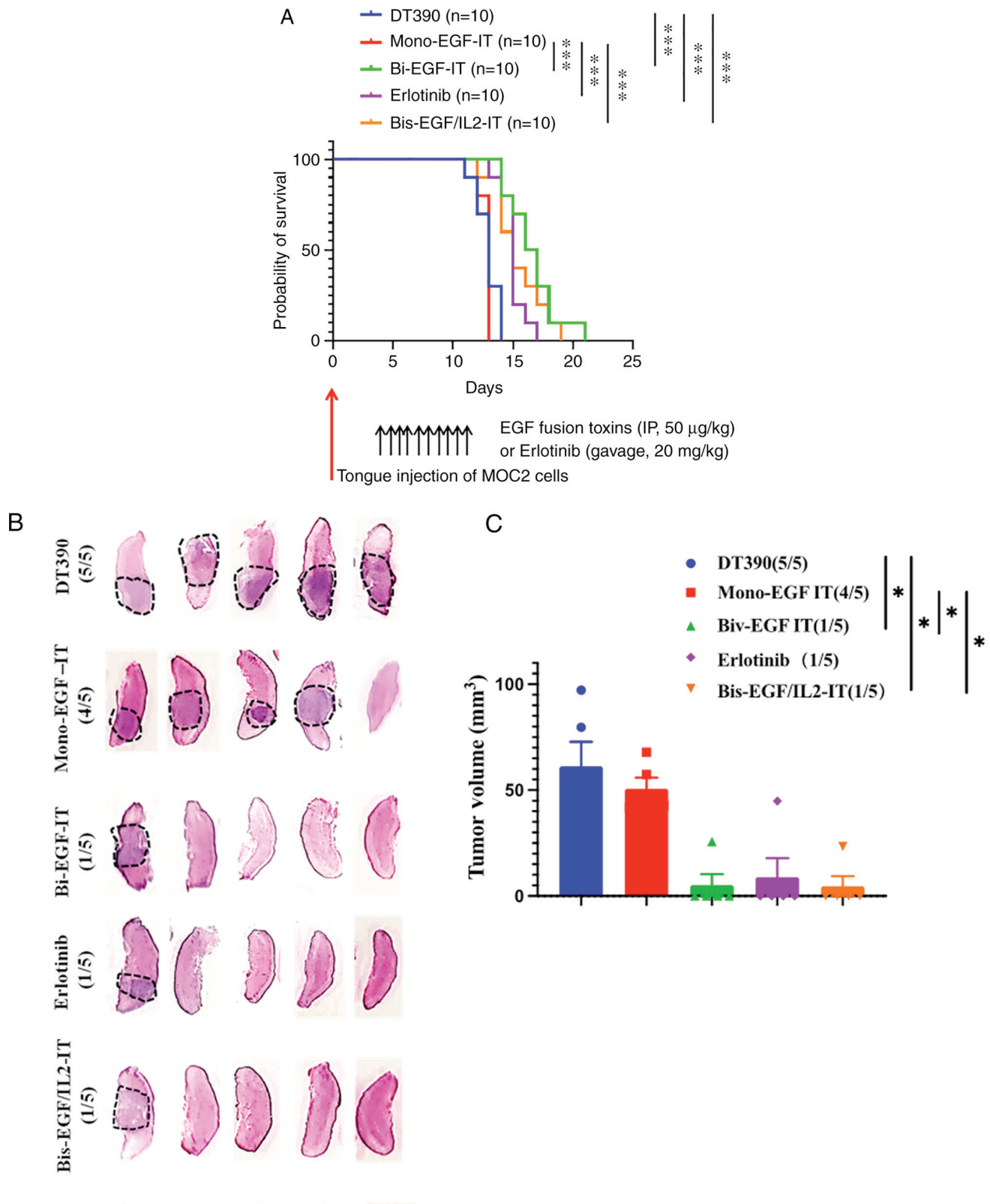


Figure 5. Antitumor efficacy of the three EGF fusion toxins against a syngeneic orthotopic tongue SCC mouse model. (A) Kaplan-Meier survival curves for mice with tongue SCC following treatment with the three EGF fusion toxins. EGFR⁺ HNSCC MOC2 cells were injected into the tongue of C57BL/6 mice on day 0. Tumor-bearing mice were treated with DT390 (negative control, blue, n=10), mono-EGF-IT (red, n=10), bi-EGF-IT (green, n=10), bis-EGF/IL2-IT (orange, n=10), or erlotinib (positive control, purple, n=10) once daily for ten consecutive days starting on day 4 after tumor cell injection. The timeline and detailed schedules for tumor cell injection and treatments are shown under the survival curves. The vertical arrows indicate the days the tumor cells (red) or treatments (black) were administered. (B) Histological images of tongues with SCC following treatment with the three EGF fusion toxins. The tongue SCCs are circled with black dotted lines. The incidence of tongue SCC is shown in parentheses. Murine EGFR⁺ HNSCC MOC2 cells were injected into the tongues of a second cohort of C57BL/6 mice and treated with DT390, mono-EGF-IT, bi-EGF-IT, bis-EGF/IL2-IT, or erlotinib (n=5 for each group). The mice were euthanized, and the tongues were harvested on day 9 after tumor cell injection. (C) Quantification of total tumor volume for each treatment group. The incidence of tongue SCC is shown in parentheses. *P<0.05 and ***P<0.001. SCC, squamous cell carcinoma; HNSCC, head and neck squamous cell carcinoma; IT, immunotoxin.

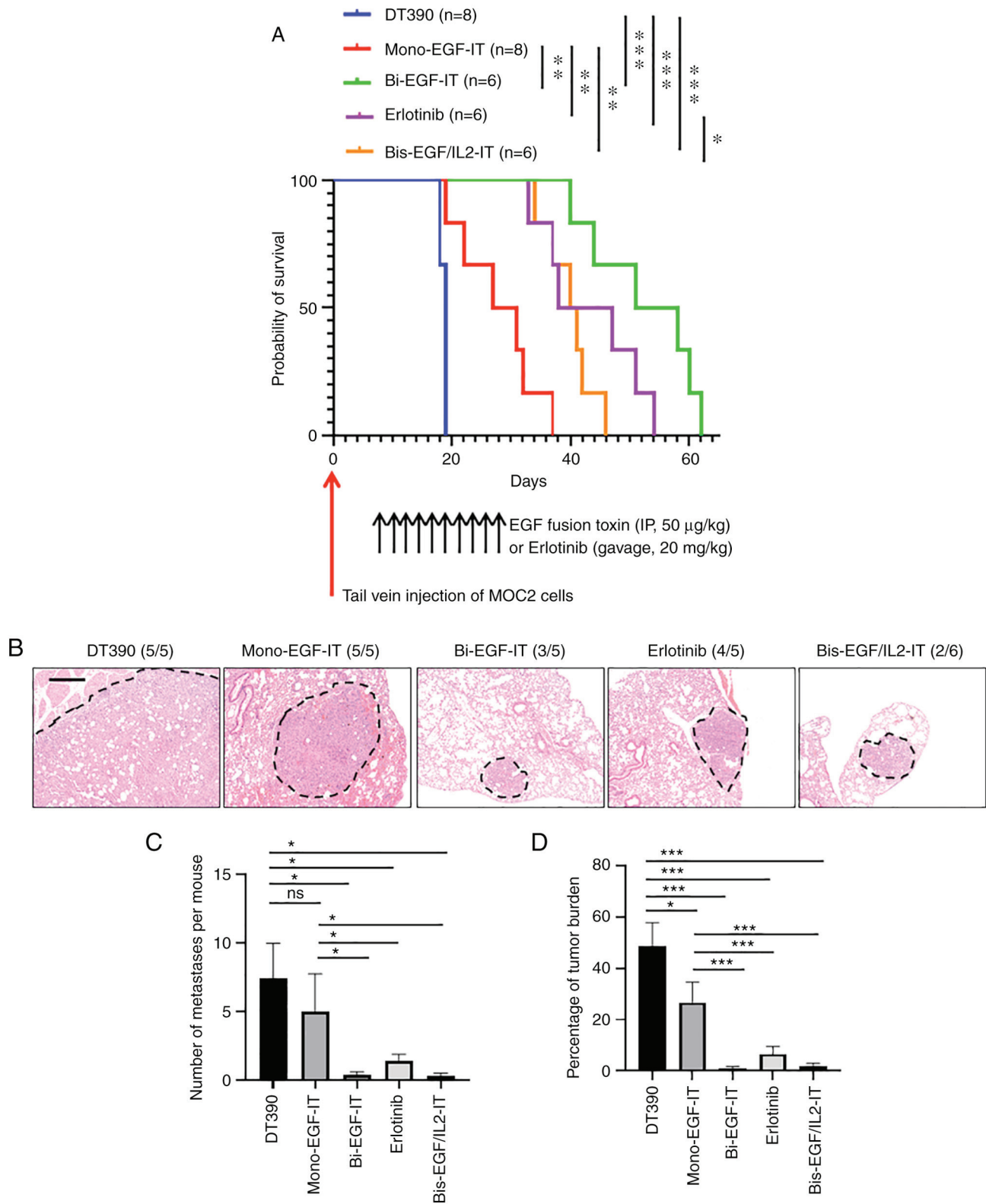


Figure 6. *In vivo* efficacy of the 3 EGF fusion toxins against lung metastasis in a syngeneic mouse model. (A) Kaplan-Meier survival curves for mice with lung metastasis following treatment with the three EGF fusion toxins. Murine EGFR⁺ HNSCC MOC2 cells were intravenously injected into C57BL/6 mice via the tail vein, and the mice were then treated with DT390 (blue, n=8), mono-EGF-IT (red, n=8), bi-EGF-IT (green, n=6), bis-EGF/IL2-IT (orange, n=6), or erlotinib (purple, n=6) once daily for 10 consecutive days starting on day 10 after tumor cell injection. The timeline and detailed schedules for tumor cell injection and treatments are shown under the survival curves. The vertical arrows indicate the days the tumor cells (red) or treatments (black) were administered. (B) Histological images of lung metastases following treatment with the 3 EGF fusion toxins or erlotinib. The lung metastases are circled with black dotted lines. The incidence of metastases is shown in parentheses. Murine EGFR⁺ HNSCC MOC2 cells were intravenously injected into C57BL/6 mice via the tail vein of a second cohort of C57BL/6 mice and treated with DT390 (n=5), mono-EGF-IT (n=5), bi-EGF-IT (n=5), bis-EGF/IL2-IT (n=6), or erlotinib (n=5). The mice were euthanized, and the lungs were harvested on day 18 after the tumor cell injection. Scale bar, 100 μ m. (C) Quantification of the number of lung metastases per mouse. (D) Quantification of the percentage of lung metastatic tumor burden per microscopic field per mouse. A total of 3 microscopic fields at x5 magnification were used to calculate the percentage of tumor occupied in each microscopic field. ns=non-significant; *P<0.05, **P<0.01 and ***P<0.001. HNSCC, head and neck squamous cell carcinoma; IT, immunotoxin.

(Fig. S1A). Necropsy of mice treated with mono-EGF-IT revealed moderate amounts of hemorrhagic fluid throughout the abdominal cavity. The stomach and duodenum were mildly distended with ingesta, while the remainder of the intestines was relatively empty except for multifocal regions of dark ingesta. The liver was diffusely pale and enlarged. The kidneys were diffusely and bilaterally pale. By contrast, the kidneys, liver, heart, and gastrointestinal organs were macroscopically normal in mice treated with either bi-EGF-IT or bis-EGF/IL2-IT (Fig. S1B).

Discussion

In the present study, our previous work was extended evaluating the efficacy and toxicity of mono-EGF-IT and bi-EGF-IT (26) to immunocompetent HNSCC mouse models. In addition, a novel fusion toxin, bis-EGF/IL2-IT, was generated to allow targeting of the tumor and its immune microenvironment. The results showed that all 3 EGF-IT exhibited a variety of efficacies in reducing tumor size (SC tumor), tumor incidence, tumor volume (orthotopic tongue model), lung metastasis, and prolonged survival in the syngeneic HNSCC mouse models with intact immune systems. Both bi-EGF-IT and bis-EGF/IL2-IT improved efficacies and reduced toxicity compared with mono-EGF-IT in the 3 immunocompetent syngeneic HNSCC mouse models. Bis-EGF/IL2-IT was superior in reducing tumor size compared with bi-EGF-IT, whereas the latter was superior to the former in prolonging survival days in the metastatic model. It was hypothesized that the immunotherapy function of bis-EGF/IL2-IT may be more effective in reducing tumor size, and the improved targeted therapy function of bi-EGF-IT may be more effective in inhibiting metastasis to prolong the survival in the metastatic model. Nonetheless, these data indicated that both bi-EGF-IT and bis-EGF/IL2-IT are more potent and less toxic than mono-EGF-IT.

The superiority of bi-EGF-IT over mono-EGF-IT is consistent with a previous study by the authors testing the efficacy and toxicity of these 2 fusion toxins in immunocompromised HNSCC mouse models (26). The improved binding affinity of the bivalent version may be one reason for this observed difference. Notably, the bis-EGF/IL2-IT performed nearly equivalent to bi-EGF-IT in efficacy and toxicity. Bis-EGF/IL2-IT was developed to examine the hypothesis that targeting both tumor and immune microenvironment could improve the efficacy. Indeed, bis-EGF/IL2-IT was more efficacious than mono-EGF-IT. HNSCC, either HPV⁺ or HPV⁻, is one of the cancer types with the highest infiltration of Tregs, which significantly contributes to immune suppression in the tumor microenvironment (36). Targeting IL2 receptor boosts the antitumor immune response via Treg depletion, as reported for a study using the FDA-approved Ontak[®] (human IL2 fusion toxin) (37) and shown in a previous study by the authors (38).

Initially, the murine EGF fusion toxins was planned to make for the studies in the syngeneic mouse tumor models. However, since the human EGF fusion toxins could bind to the murine EGFR⁺ MOC2 tumor cells, it was decided to directly assess the *in vitro* and *in vivo* efficacy of human EGF fusion toxins against murine EGFR⁺ HNSCC MOC2 tumor cells.

The limitation and future direction of the present study are as follows: i) Although the syngeneic HNSCC mouse model is immunocompetent, the cell line used is derived from murine

experimental HNSCC model, which has the limitation of human relevance. A humanized HNSCC mouse model, which allows assessing human HNSCC cell lines or cell lines from patient-derived xenograft in the immunocompetent environment, will be ideal to address both human relevance and immunocompetent microenvironment; ii) Although bis-EGF/IL2-IT demonstrated the best *in vivo* efficacy, the *in vitro* efficacy was not as well as expected. It was hypothesized that, except for the EGF-based targeted therapy function, IL2 domain of bis-EGF/IL2-IT may also stimulate immune response and deplete tumor-infiltrating effector Tregs *in vivo*. However, the *in vitro* efficacy assay may only detect the targeted therapy function, not the immunotherapy function of bis-EGF/IL2-IT; iii) The effect of bis-EGF/IL2-IT on tumor microenvironment is hypothetical. A comprehensive characterization of tumor microenvironment will mechanistically support the hypothesis and is warranted; iv) There was only one murine OSCC cell line available for use in the present study. Although expressed, the EGFR levels in the MOC2 cell line may not be high enough to observe an improved response to the treatment efficacy of the human EGF fusion toxins. More syngeneic murine HNSCC models with a variety of EGFR expression levels may provide more information on EGFR expression in response to treating human EGF fusion toxins in HNSCC mouse models in the presence of host immunity; v) Given the superiority of bi-EGF-IT and bis-EGF/IL2-IT over mono-EGF-IT, a combination of bivalent and bispecific approaches should enhance both binding and the anticancer immune response and may further improve the performance of EGF-IT in the treatment of HNSCC.

In summary, a novel bis-EGF/IL2-IT was generated and its efficacy and toxicity were examined, together with mono-EGF-IT and bi-EGF-IT, in the treatment of syngeneic HNSCC mouse models with intact immune systems. Both bis-EGF/IL2-IT and bi-EGF-IT were more effective and less toxic than mono-EGF-IT, suggesting that targeting the immune microenvironment or enhancing binding affinity to EGF will improve the performance of EGF-IT in the treatment of HNSCC mouse models.

Acknowledgements

Not applicable.

Funding

No funding was received.

Availability of data and materials

The datasets used and/or analyzed during the current study are available from the corresponding authors upon a reasonable request.

Authors' contributions

YQ, SLL and ZhiW designed the experiments. YQ, ZQ, ZhaW, YC, LL and HZ performed the experiments. YQ, DM, EAP, SLL and ZhiW analyzed and interpreted the data. YQ, DM, EAP, SLL and ZhiW wrote and reviewed the manuscript. All

authors read and approved the final manuscript. YQ, SLL and ZhiW confirmed the authenticity of all the raw data.

Ethics approval and consent to participate

The animal experiments were approved (approval no. 00866) by the Institutional Animal Care and Use Committee (IACUC) of the University of Colorado Anschutz Medical Campus (Aurora, USA).

Patient consent for publication

Not applicable.

Competing interests

ZhiW is the founder of Rock Immune LLC. The remaining authors declare that they have no competing interests.

References

1. Chow LQM: Head and neck cancer. *N Engl J Med* 382: 60-72, 2020.
2. Siegel RL, Miller KD and Jemal A: Cancer statistics, 2020. *CA Cancer J Clin* 70: 7-30, 2020.
3. Wyss A, Hashibe M, Chuang SC, Lee YC, Zhang ZF, Yu GP, Winn DM, Wei Q, Talamini R, Szeszenia-Dabrowska N, *et al*: Cigarette, cigar, and pipe smoking and the risk of head and neck cancers: Pooled analysis in the International head and neck cancer epidemiology consortium. *Am J Epidemiol* 178: 679-690, 2013.
4. Chaturvedi AK, Engels EA, Pfeiffer RM, Hernandez BY, Xiao W, Kim E, Jiang B, Goodman MT, Sibug-Saber M, Cozen W, *et al*: Human papillomavirus and rising oropharyngeal cancer incidence in the United States. *J Clin Oncol* 29: 4294-4301, 2011.
5. Gillison ML, Chaturvedi AK, Anderson WF and Fakhry C: Epidemiology of human papillomavirus-positive head and neck squamous cell carcinoma. *J Clin Oncol* 33: 3235-3242, 2015.
6. Pfister DG, *et al*: NCCN clinical practice guideline in oncology-head and neck cancers, version 1. 2019-March 6, 2019, 2019.
7. Cramer JD, Burtneff B, Le QT and Ferris RL: The changing therapeutic landscape of head and neck cancer. *Nat Rev Clin Oncol* 16: 669-683, 2019.
8. Cramer JD, Burtneff B and Ferris RL: Immunotherapy for head and neck cancer: Recent advances and future directions. *Oral Oncol* 99: 104460, 2019.
9. NCI, SEER Database: Cancer Stat Facts: Oral cavity and pharynx cancer, laryngeal cancer, 2009-2015.
10. Cohen EEW, LaMonte SJ, Erb NL, Beckman KL, Sadeghi N, Huthcheson KA, Stubblefield MD, Abbott DM, Fisher PS, Stein KD, *et al*: American cancer society head and neck cancer survivorship care guideline. *CA Cancer J Clin* 66: 203-239, 2016.
11. Pulte D and Brenner H: Changes in survival in head and neck cancers in the late 20th and early 21st century: A period analysis. *Oncologist* 15: 994-1001, 2010.
12. Kalyankrishna S and Grandis JR: Epidermal growth factor receptor biology in head and neck cancer. *J Clin Oncol* 24: 2666-2672, 2006.
13. Bossi P, Resteghini C, Paielli N, Licita L, Pilotti S and Perrone F: Prognostic and predictive value of EGFR in head and neck squamous cell carcinoma. *Oncotarget* 7: 74362-74379, 2016.
14. Trivedi S and Ferris RL: Epidermal growth factor receptor-targeted therapy for head and neck cancer. *Otolaryngol Clin North Am* 54: 743-749, 2021.
15. Forastiere AA and Burtneff BA: Epidermal growth factor receptor inhibition in head and neck cancer-more insights, but more questions. *J Clin Oncol* 25: 2152-2155, 2007.
16. Saba NF, Chen ZG, Haigentz M, Bossi P, Rinaldo A, Rodrigo JP, Mäkitie AA, Takes RP, Stojan P, Vermorken JB and Ferlito A: Targeting the EGFR and immune pathways in squamous cell carcinoma of the head and neck (SCCHN): Forging a new alliance. *Mol Cancer Ther* 18: 1909-1915, 2019.
17. Muratori L, La Salvia A, Sperone P and Di Maio M: Target therapies in recurrent or metastatic head and neck cancer: State of the art and novel perspectives. A systematic review. *Crit Rev Oncol Hematol* 139: 41-52, 2019.
18. Sharafinski ME, Ferris RL, Ferrone S and Grandis JR: Epidermal growth factor receptor targeted therapy of squamous cell carcinoma of the head and neck. *Head Neck* 32: 1412-1421, 2010.
19. Bardelli A and Jänne PA: The road to resistance: EGFR mutation and cetuximab. *Nat Med* 18: 199-200, 2012.
20. Jelinek MJ and Vokes EE: Epidermal growth factor receptor blockade in head and neck cancer: What remains? *J Clin Oncol* 37: 2807-2814, 2019.
21. Byeon HK, Ku M and Yang J: Beyond EGFR inhibition: Multilateral combat strategies to stop the progression of head and neck cancer. *Exp Mol Med* 51: 1-14, 2019.
22. Saada-Bouid E and Le Tourneau C: Beyond EGFR targeting in SCCHN: Angiogenesis, PI3K, and other molecular targets. *Front Oncol* 9: 74, 2019.
23. Pastan I, Hassan R, Fitzgerald DJ and Kreitman RJ: Immunotoxin therapy of cancer. *Nat Rev Cancer* 6: 559-565, 2006.
24. Kim JS, Jun SY and Kim YS: Critical issues in the development of immunotoxins for anticancer therapy. *J Pharm Sci* 109: 104-115, 2020.
25. Akbari B, Farajnia S, Ahdi Khosroshahi S, Safari F, Yousefi M, Dariushnejad H and Rahbarnia L: Immunotoxins in cancer therapy: Review and update. *Int Rev Immunol* 36: 207-219, 2017.
26. Qi Z, Qiu Y, Wang Z, Zhang H, Lu L, Liu Y, Mathes D, Pomfret EA, Gao D, Lu SL and Wang Z: A novel diphtheria toxin-based bivalent human EGF fusion toxin for treatment of head and neck squamous cell carcinoma. *Mol Oncol* 15: 1054-1068, 2021.
27. Onda M, Kobayashi K and Pastan I: Depletion of regulatory T cells in tumors with an anti-CD25 immunotoxin induces CD8 T cell-mediated systemic antitumor immunity. *Proc Natl Acad Sci USA* 116: 4575-4582, 2019.
28. Raeber ME, Sahin D and Boyman O: Interleukin-2-based therapies in cancer. *Sci Transl Med* 14: eabo5409, 2022.
29. Liu YY, Woo JH and Neville DM: Targeted introduction of a diphtheria toxin resistant mutation into the chromosomal EF-2 locus of *Pichia pastoris* and expression of immunotoxin in the EF-2 mutants. *Protein Expr Purif* 30: 262-274, 2003.
30. Judd NP, Winkler AE, Murillo-Sauca O, Brotman JJ, Law JH, Lewis JS Jr, Dunn GP, Bui JD, Sunwoo JB and Uppaluri R: ERK1/2 regulation of CD44 modulates oral cancer aggressiveness. *Cancer Res* 72: 365-374, 2012.
31. Peraino JS, Schenk M, Li G, Zhang H, Farkash EA, Sachs DH, Huang CA, Duran-Struuck R and Wang Z: Development of a diphtheria toxin-based recombinant porcine IL-2 fusion toxin for depleting porcine CD25⁺ cells. *J Immunol Methods* 398-399: 33-43, 2013.
32. Zheng Q, Wang Z, Zhang H, Huang Q, Madsen JC, Sachs DH, Huang CA and Wang Z: Diphtheria toxin-based anti-human CD19 immunotoxin for targeting human CD19⁺ tumors. *Mol Oncol* 11: 584-594, 2017.
33. Fletcher EV, Love-Homan L, Sobhakumari A, Feddersen CR, Koch AT, Goel A and Simons AL: EGFR inhibition induces proinflammatory cytokines via NOX4 in HNSCC. *Mol Cancer Res* 11: 1574-1584, 2013.
34. Stanam A, Gibson-Corley KN, Love-Homan L, Ihejirika N and Simons AL: Interleukin-1 blockade overcomes erlotinib resistance in head and neck squamous cell carcinoma. *Oncotarget* 7: 76087-76100, 2016.
35. Du L, Chen X, Cao Y, Lu L, Zhang F, Bornstein S, Li Y, Owens P, Malkoski S, Said S, *et al*: Overexpression of PIK3CA in murine head and neck epithelium drives tumor invasion and metastasis through PDK1 and enhanced TGFβ signaling. *Oncogene* 35: 4641-4652, 2016.
36. Mandal R, Şenbabaoğlu Y, Desrichard A, Havel JJ, Dalin MG, Riaz N, Lee KW, Ganly I, Hakimi AA, Chan TA and Morris LG: The head and neck cancer immune landscape and its immunotherapeutic implications. *JCI Insight* 1: e89829, 2016.
37. Kumar P, Kumar A, Parveen S, Murphy JR and Bishai W: Recent advances with Treg depleting fusion protein toxins for cancer immunotherapy. *Immunotherapy* 11: 1117-1128, 2019.
38. Wang Z, Zheng Q, Zhang H, Bronson RT, Madsen JC, Sachs DH, Huang CA and Wang Z: Ontak-like human IL-2 fusion toxin. *J Immunol Methods* 448: 51-58, 2017.



This work is licensed under a Creative Commons Attribution-NonCommercial-NoDerivatives 4.0 International (CC BY-NC-ND 4.0) License.